crystals

MDPI

Article

Influence of Pyruvic Acid and UV Radiation on the Morphology of Silica-carbonate Crystalline Biomorphs

Karina S. Pérez and Abel Moreno *

Instituto de Química, Universidad Nacional Autónoma de México. Avenida Universidad 3000. Col. UNAM. C.P. 04510 Ciudad de Mexico, Mexico; ianaks000@gmail.com

* Correspondence: carcamo@unam.mx; Tel.: +52-55-5622-4467

Received: 18 December 2018; Accepted: 27 January 2019; Published: 28 January 2019

Abstract: In this work we report the effect of introducing pyruvic acid (PA) in the growing process of silica-carbonate biomorphs. Gas-diffusion and single-phase methods were performed, and different concentrations of pyruvic acid were tested. Moreover, influence of UV radiation on the morphogenesis of the samples was analyzed. Since PA decomposes in CO_2 and other compounds under UV radiation, here we demonstrate that PA decomposition enables a source of carbonate ions to induce the precipitation of silica-carbonate biomorphs in absence of environmental CO_2. We also found that high concentrations [0.5 M] of PA inhibit the formation of biomorphs, while lower concentrations [0.01 M] results in common life-like structures. However [0.1 M] of PA provokes the precipitation of carbonates of alkaline earth metals in non-usual crystalline habits, i.e., semi-spherical smoothed shapes sized between 10 and 70 μm and homogeneously growth on a glass substrate.

Keywords: silica-carbonate biomorphs; pyruvic acid; diffusion-reaction synthesis; induced morphology crystalline aggregates

1. Introduction

"Worm-like", cardioid sheets and helical fossilized microstructures, among others, are thought to be the indicium of ancient type of cyanobacterial microorganisms from the Precambrian age [1,2]. The origin of life has been dated considering that these morphologies can be constructed solely by living organisms [3,4]. As it is well known, living organisms are able to fabricate biogenic minerals usually in the presence of biomolecules [5,6]; however, it has been demonstrated that complex crystalline long-range symmetry structures with similar morphologies can be synthetized under purely inorganic reactions by inducing the precipitation of carbonates or silica-carbonates in an alkaline medium [7–9], which resembles atmospheric conditions in an early stage of the Earth's life. These inorganic *life-like* microstructures have been named biomorphs, which are peculiar because of its astonishing curvatures out of the classical crystalline mineral features. Since their discovery in the early 1980's by García-Ruiz et al., a vast research has been conducted in this field, which has encouraged the growth of biomorphs in a variety of controlled morphologies, and through different techniques, i.e., *reaction-diffusion*, *gas-diffusion* and *single-phase* methods [10–13]. In all cases the basic principle implies the precipitation of alkaline earth metal salts in a rich carbonated medium. In the reaction-diffusion method, the main advantage is the non-convective controlled pathway to which precipitation reactions are subjected [10,14]. This is achieved because the alkaline gel serves as a matrix of diffusion, resulting in biomorphs growing as long as few millimeters in size. However, growing biomorphs in gel results in a complicated manipulation of the structures because, in order to characterize them, we need to remove the gel matrix. This is performed by dissolving the gel matrix in NaOH. However, gel method allows

the formation of larger and more abundant structures, favoring helical structures over "worm-like". This has been mostly observed in sol conditions. A detailed explanation of these phenomena can be found in reference [14]. In the gas-diffusion method, biomorphs are grown in solution. In this case, a substrate of glass, aluminum, gold, etc., can be adequately set into the sol, allowing biomorphs to grow on the surface of the substrate. Carbonate precipitation is led by CO_2 diffusion from environment. Similarly, single-phase method is based in a sol procedure where CO_3^{2-} ions are added to the solution, and the container is perfectly sealed to avoid interactions with outer compounds. The latter method is advantageous since carbonate ion concentration does not depend on the environmental conditions; hence, it is not affected by chemical gradients. Although this improves reproducibility; it takes a bit longer to observe first signs of biomorphs formation [12].

Extensive research has been conducted in order to study biomorphs morphogenesis. For example, proteins related with biomineralization processes of sea specimens [15], silane co-condensation, metal nanoparticles and quantum dots, organic polymerization [16] and even formamide [17], which led to the formation of complex prebiotic molecules, are some of the approaches that evaluate morphogenic changes or functionalization in silica-carbonate precipitates. Despite this, few studies have been focused on the introduction of prebiotic molecules during or after the process of biomorph growth.

In this work we analyzed the influence of pyruvic acid in the morphogenesis of biomorphs. PA is an *α-keto acid* that acts as an intermediary in the metabolism of carbohydrates, proteins and fats, and serves as a biological fuel in both aerobic and anaerobic processes since it is involved in Krebs cycle and glycolysis. It is also known that under hydrothermal conditions it produces a mixture of high complexity of organic molecules of high molecular weight; therefore, it is presumed to be an important reactant in primitive metabolic pathways [18]. Moreover, it has been demonstrated that PA degrades via photolysis [19]. Aqueous and gas phases of PA have been exposed to UV radiation, and diverse photochemical pathways have been proposed for its degradation. However, in all cases, the formation of carboxyl radicals and CO_2 is observed [20–22]. Therefore, here it is hypothesized that PA could serves as a precursor in the precipitation of carbonates if it is simulated a non-oxidant atmosphere exposed to UV radiation.

2. Materials and Methods

Silica-carbonate biomorphs were obtained following the gas-diffusion and single-phase methods reported elsewhere [10,13]. Ba and Sr were used in their chloride form to induce metal carbonate precipitates. Growth of biomorphs by gas-diffusion method took place in an alkaline solution where pH was adjusted to 11 $\pm$ 0.1 with NaOH 1 M. A slide of glass (~5 $\times$ 5 mm) was set vertically into a 1:1:0.1 aqueous salt (i.e. $M^{2+}Cl_2^{-1}$ with M^{2+} = Ba or Sr, 20 mM), sodium metasilicate (~1000 ppm Si) and PA (0.01, 0.1 and 0.5 M) solution by volume. The reaction vessel was slightly covered to allow CO_2 diffusion from the environment (Figure 1a). After 24 h the glass slide was removed from the solution and carefully rinsed with deionized (DI) water and acetone for 3 min to reduce capillarity stress during drying at room temperature. Samples obtained by this procedure were monitored as control samples.

UV radiation influence on the growth of silica-carbonate precipitates was analyzed from the results of two different experiments. In the first, we followed the exact same procedure as previously described above; however, before mixing the reactants they were bubbled with nitrogen and then placed into a sealed container (Figure 1b) to avoid both, pre-dissolved and environmental CO_2 respectively. This system simulates a single-phase method to growth biomorphs.

In the second experimental configuration, we prepared a solution 1:1 of $M^{2+}Cl_2^{-1}$:Na_2SiO_3 (by volume). The reaction vessel with the solution and the glass slide was placed into a sealed crystallization mushroom containing 2 ml of PA [0.1 M] at the bottom (Figure 1c).

In both last cases (Figure 1b,c), the pH was adjusted to 11 $\pm$ 0.1. An UV lamp was placed 10 cm above the reaction vessels to irradiate them for 24 h. Previously, absorbance measurements of PA were carried out to identify the right wavelength range for its photolysis.

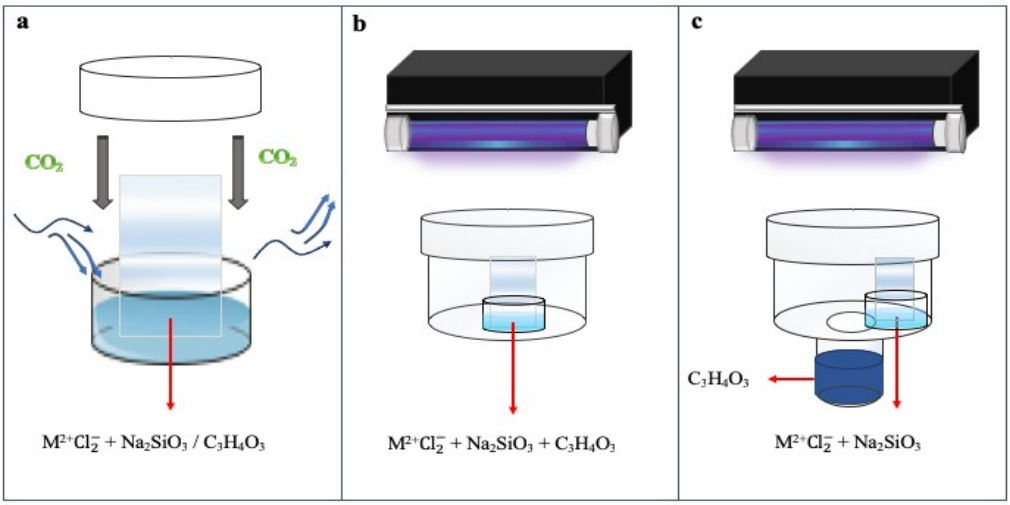

Figure 1. Schematic representation of the biomorphs growth systems. (**a**) Gas-diffusion method. (**b**) Single-phase method under UV radiation. (**c**) Gas-diffusion method under UV radiation. M = Ba or Sr.

3. Characterization

Optical images were obtained with a SZH10 OLYMPUS microscope (OLYMPUS OPTICAL CO. LTD, Osachi-shibamiya, Okaya Nagano, Japan). Scanning electron microscopy was carried out with a SEM-TESCAN VEGA3 SB microscope (TESCAN Brno, s.r.o., Brno, Czech Republic) operating at 15 keV in back scattering electron (BSE) mode (all samples were gold-coated to improve conductivity). Raman spectra and imaging were acquired with a confocal Raman microscope WITec Alpha 300R system operating at room temperature with a Nd:YVO_4 laser (WITEC Instruments Corp., Knoxville, TN, USA) (532 nm) at 14 mW and the spectral resolution of the spectrometer is 4–5 cm^{-1}. Absorbance was obtained with a Thermo Scientific BioMate 3. UV radiation was carried out with an UVP lamp UVLMS-38, 8 Watts (Analytik Jena LLC, Upland, CA, USA) operating at medium wavelength (302 nm). EDS measurements were acquired with a HRSEM JEOL 7800F (JEOL Ltd., Tokyo, Japan) operating at a 15 kV.

4. Results and discussion

4.1. Gas Diffusion Experiment with PA

SEM images in Figure 2 show control samples of barium silica-carbonate precipitates with and without PA added (following the experimental set up shown in Figure 1a). In Figure 2a–c, it is presented the images from control samples with no PA added. In there, cardioid sheets, worms, helices and a combination of them are presented.

Biomorphs synthetized with [0.01 M] of PA presented a similar morphology to those with no PA (Figure 2d–f). When using [0.5 M] PA, no crystallization was observed (no precipitates were found). Nevertheless, [0.1 M] PA had a strong influence in the morphology of biomorphs, as can be seen for $BaCO_3$ precipitates in Figure 2g–i, where only spherical and semispherical structures were present, all of them sized between 10 and 70 μm of diameter. Similar results were found when using strontium (Supplementary materials, Figure S1). These images illustrate crystals' alignment, but also the amorphous SiO_2 alternated with $BaCO_3$ co-precipitation (Figure 2h).

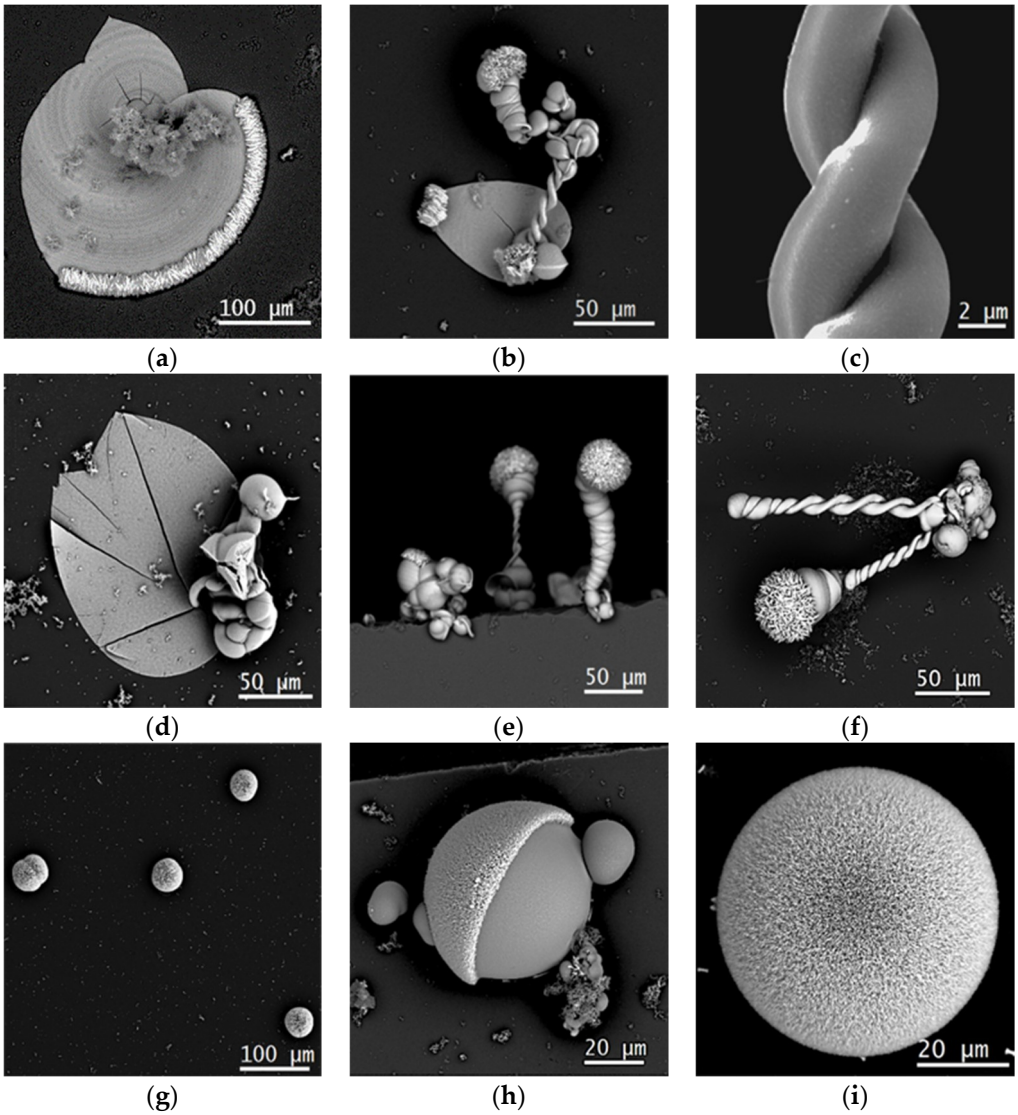

Figure 2. Scanning electron microscopy images of Ba silica-carbonates. (**a–c**) Control structures with no PA; (**d–f**) Structures synthetized with [0.01 M] PA; (**g–i**) Structures synthetized with [0.1 M] PA where spherical and semispherical morphologies were found.

Energy dispersive spectroscopy (EDS) analysis was performed in order to identify if it is Ba or Si the one that has specific distribution over the samples, particularly in those structures where different geometries were observed. Results showed that Ba and C are mostly present where crystals arrangements are clearly visible. When a structure shows an outwardly planar zone, for example sheets or helices surfaces, an apparently higher concentration of Si is found. Notice that high resolution SEM images had previously demonstrated that biomorphs smoothed surfaces present an arrangement of aligned nanorods on the surface. However, when analyzing spherical structures, the distribution appears relatively homogeneous over the sample (Supplementary materials, Figure S2). Furthermore, similar proportions of Ba and Si were found among control samples and those synthetized in gas diffusion and single-phase experimental configuration, so that, complementary analysis of the distribution of compounds in the sample is needed. In order to do this, we run measurements with confocal-Raman microscopy. This technique allowed us to observe the distribution of $BaCO_3$ on the sample and get punctual spectra over specific regions of the structures. Since biomorphs were synthetized on glass substrates, a clear differentiation between amorphous SiO_2 from the sample and SiO_2 from the glass substrate was not fully accomplished. However, it can be faintly distinguished

in the mapping. In Figure 3a, we observe the Raman spectrum of the control sample. It is worth mentioning that spectra of different regions of the structures were acquired, i.e., from the planar sheet zones, from the worm-like and helical regions; however, there were not significant variations. The characteristic peaks previously reported from witherite ($BaCO_3$), showed almost total coincidence with the acquired spectra. The peaks at 132.2, 151.4, 178.8 and 227.4 cm^{-1} are associated to CO_3^{2-} rotational and translational modes; 693.2 cm^{-1} and 1062.1 cm^{-1} corresponding to O-C-O bindings in an out of plane bending, respectively; and 1419.4 cm^{-1} and 1506.1 cm^{-1} for a C-O stretching [23]. In Figure 3b we observe the mapping of the sample, where (i) corresponds to the optical image of the structure; (ii) corresponds to the monitoring of 1062.1 cm^{-1} peak; and (iii) corresponds to one of the glass substrate band at 1100 cm^{-1}, (Supplementary materials, Figure S3).

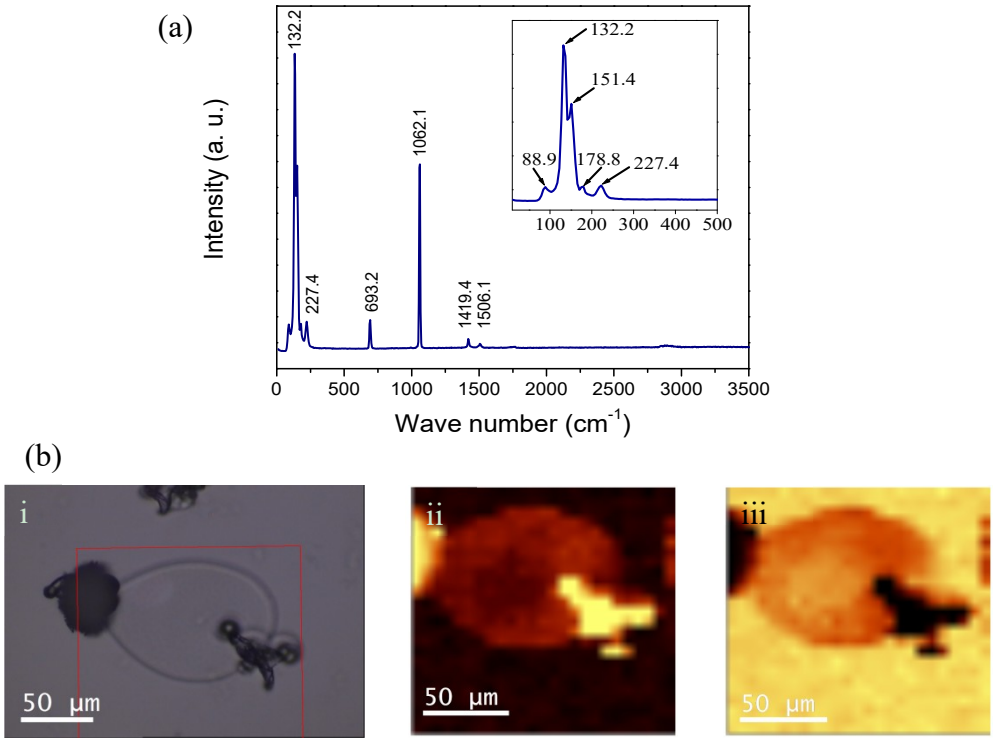

Figure 3. (**a**) Raman spectrum, and (**b**) confocal images of a Ba-synthetized biomorph; (i) optical image from the sample; (ii) Mapping of the 1062.1 cm^{-1} shift for $BaCO_3$; (iii) Mapping of the glass substrate tracked at 1100 cm^{-1}.

Despite of the prominent variations on morphology, as seen in Figure 2, the Raman shifts appeared mostly in the same positions in samples with and without PA. However, minimum variations were observed, i.e., the intensity of the peaks at 132 and 151 cm^{-1} is inverted, the peak at 179 cm^{-1} in Figure 3 does not appear anymore, and there is slight shift from 227 to 218 cm^{-1} and from 693 to 688 cm^{-1}. Furthermore, in Figure 4 peaks at 932 and 2929 cm^{-1} were observed, which are not recognizable for $BaCO_3$ but could be attributed to the presence of PA as can be seen in reference [24]. Since the peak at 932 cm^{-1} is too short, not enough resolution for mapping this peak was achieved.

Nevertheless, these changes do not prove that there is a variation in the crystalline structure of the samples. Even different reports have found similar spherical and semispherical structures at different condition when synthetizing silica-carbonates of alkaline earth elements. As it is well known, biomorphs formation proceed along a sequence of phenomenological stages, where usually some globular clusters (cauliflower or raspberry-like morphologies) evolve to laminar or cardioid sheet shapes, and at some point, they may curl to produce worm or helical morphologies [25]. However, there are some reports where globular morphologies are obtained by adding organic or inorganic molecules during the growing stage. For example, Sanchez-Puig et al. found mitotic cell-like structures

when synthetizing biomorphs in gels in the presence of biomineralization proteins, particularly when using extract of sea urchin spines [15]; Eiblmeier et al., demonstrated that spherical amorphous $BaCO_3$ core-shell-shell particles can be developed if specific high silica concentrations are added to a mix of $BaCl_2$ and $NaCO_3$ [26]; García-Ruiz et al. synthetized biomimetic minerals crystallizing $CaCO_3$ in Ney water and some of the structures they obtained consisted of vaterite spherulitic structures [27]; Ruiz-Arellano et al., observed spherical shaped calcite crystals when growth occurred in presence of intramineral proteins from eggshells of ratite birds [28]. In all cases the modification in the crystal's habits has been attributed to the non-specific adsorption of the organic/inorganic molecules (proteins, silica) on the surface of crystals, blocking its growth on every face.

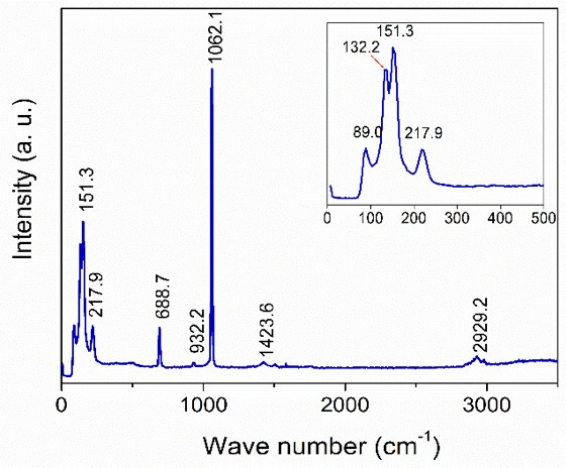

Figure 4. Raman spectrum of a Ba-synthetized biomorph in the gas diffusion method with pyruvic acid [0.1 M].

4.2. Single-phase Experiment under UV Radiation

On the other hand, it is well known that PA is photolyzed under UV radiation. The resulting compounds include CO_2 which is a primary reactant for the precipitation of alkaline earth carbonates when using the gas diffusion method. Absorbance measurements of PA showed a maximum at 318 nm, so, for the following experiments the UV lamp was set at medium wavelength. The maximum emission of the lamp in this range is 302 nm.

In the first experimental setup under UV radiation (Figure 1b), when PA was added to the mix of $M^{2+}Cl_2{}^{-1}$ and Na_2SiO_3, a single-phase system was simulated. Since CO_2 is not allowed to diffuse from the environment, the formation of precipitates should be led only by $CO_3{}^{2-}$ ions produced due to the photolysis of PA. Other single-phase experiments for biomorphs formation have been proposed by Nakouzi et al. [29]. In their experiments, atmospheric CO_2 diffusion is excluded, and $CO_3{}^{2-}$ ions are added to the sol by incorporating dissolved sodium carbonate to the mix, and the resulting structures show indistinguishable features from those obtained by gas-diffusion methods. However, our results with [0.1 M] PA and under UV radiation did not show that classical morphologies; instead, it was only found spherical and semispherical precipitates like those found when PA was added but no UV radiation was involved in the gas diffusion experiments (Figure 5).

The Raman spectrum of the structures obtained by this experimental setup is shown in Figure 6 (black line). Here, the peaks at 932 and 2929 cm^{-1} observed in the gas-diffusion setup without UV radiation (Figure 4) were not observed, which result evident since PA has been degraded by the UV radiation.

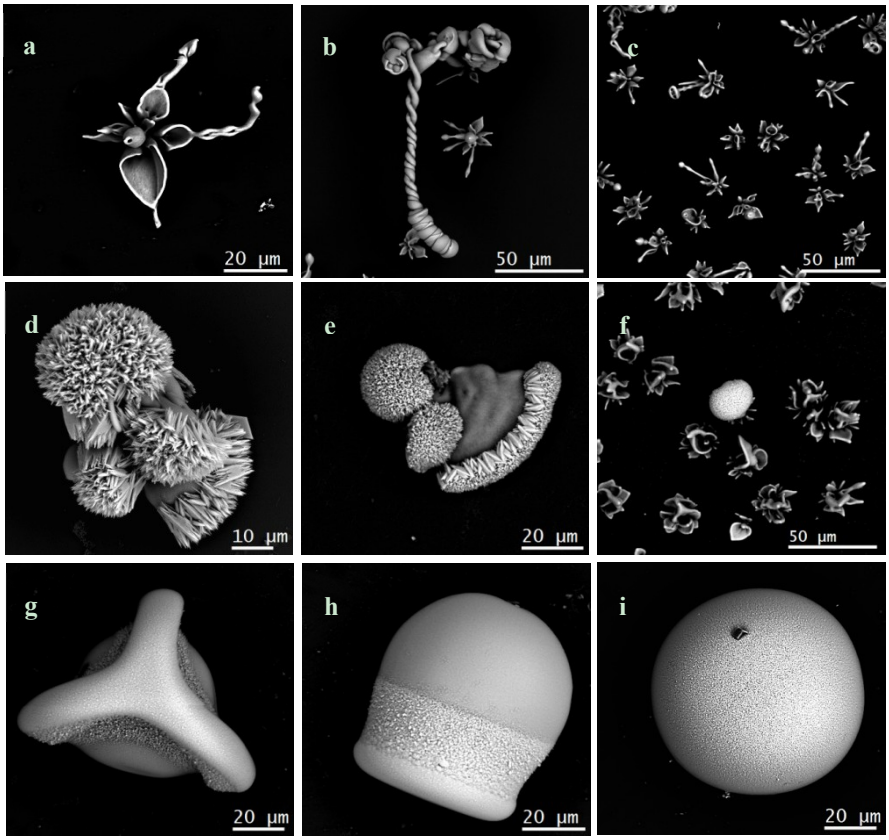

Figure 5. Flower-like and helical morphologies in samples without PA added (**a–c**). Spherulitic, sheets and flower-like morphologies observed when PA is not in direct contact with reactions solutions (**d–f**). Semispherical and spherical morphologies observed when solutions are mixed with PA (**g–i**). In all cases the samples were exposed to UV radiation during 24 h.

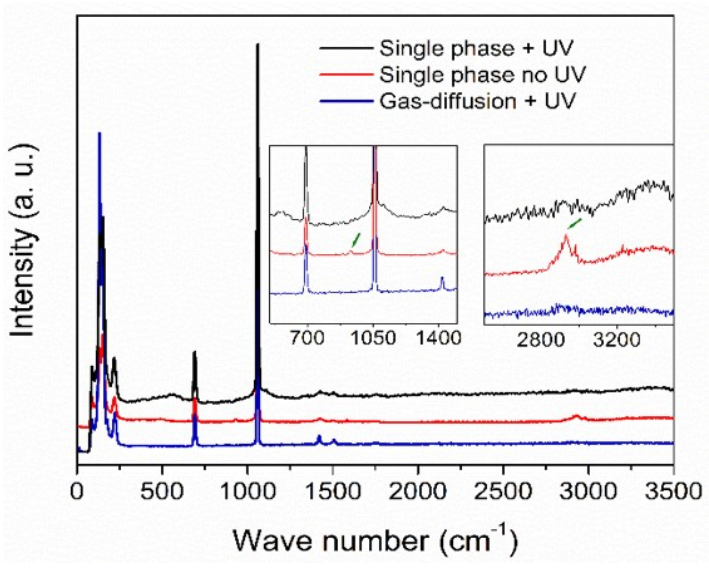

Figure 6. Raman shifts from $BaCO_3$ precipitates growth with PA [0.1 M]. Blue line: gas-diffusion setup under UV radiation. Red line: Single-phase setup without UV radiation. Black line: single-phase setup under UV radiation.

As a result of the photochemical reactions of PA, other organic compounds including acetic acid, formaldehyde, glyoxylic acid, formic acid, oxalic acid and carbon dioxide [20,30,31] are formed. It is

noticeable that most of them present a higher pH value than PA. Nevertheless, it is also highlighted that the surface of these spherical entities is smoother than in the previous experiment. A possible explanation could be that $BaCO_3$ precipitation is hindered by either the absorption of PA or derived compounds due to its photolysis, blocking the growth of the different symmetry planes, or by the variations in local pH during co-precipitation, also attributable to the presence of those compounds. However, their expected low concentration made them not easily detectable by conventional Raman spectroscopy; but even small concentrations could promote a slight decrement in the local pH and therefore, the inhibition of $BaCO_3$ precipitation.

The "worm-like", cardioid sheets, helical filaments etc., as those presented in the Figure 2c, have been used as one of the most important criteria to determine a biological and chemical origin of life. However, since purely inorganic biomorphs were synthetized, this criterion has been disregarded. Spheroidal and clustered microstructures were identified in the Strelley Pool Formation, the Farrell Quartzite and the Moodies Group. These structures can be compared with *monococci* bacterias which are sized ~10 μm. Recently, a research from Rouillard et al., concludes that it is highly unlikely that biomorphs growing from solution will produce a homogeneous population of spheroids [32]. However, in this work we demonstrated that under specific conditions, the interaction of small molecules in solution, causes the formation of a homogeneous number of spherulitic shapes (Figure 7).

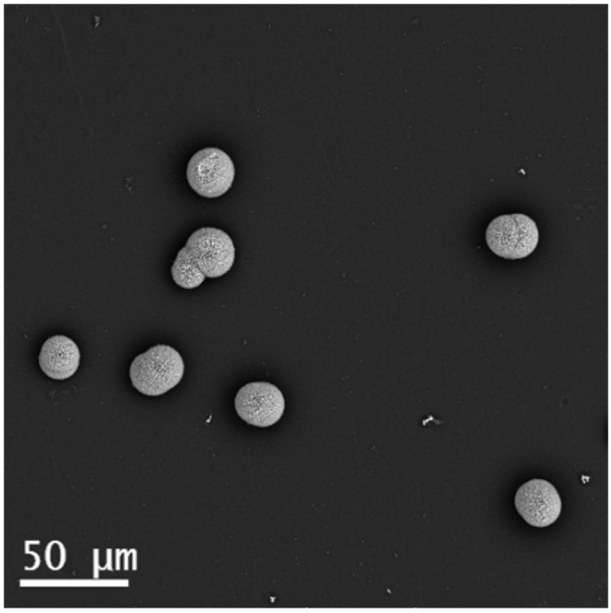

Figure 7. Spherulitic structures obtained from gas diffusion experiments for $BaCO_3$ precipitates in presence of PA [0.1 M].

4.3. Gas Diffusion Experiment under UV Radiation

In the second experimental setup (Figure 1c), control samples with no PA added were found to grow shaped as flower-like. Few sheets, worms or helical biomorphs were also observed (Figure 5a–c). As this setup does not allow CO_2 uptake from environment, the formation of the few observed structures can be attributable to minimum quantities of remaining CO_2 after bubbling or dissolving into the solution during the preparation of the samples, since they were not mixed in a controllable non-oxidant atmosphere.

When the PA was added to the bottom of the mushroom, we found a diversity of morphologies, i.e., typical biomorphs, but also spherulitic shaped structures. The last ones present a surface where crystalline arrangement can be observed (Figure 5d–f). Statistically, the number of precipitates formed with no PA/PA was >1/50. This result shows that the degradation of PA by UV radiation provides a source of CO_3^{-2} ions that enables the precipitation of $BaCO_3$ which was corroborated by acquiring the

Raman spectra of the structures (Figure 6, blue line), where the same bands as in Figure 3 were seen; therefore, no evidence of the presence of PA in the surface of the structures was observed. In contrast, no spherulitic structures were seen when PA was not involved in the process, hence, it could be speculated that some gaseous species produced by the PA degradation could be dissolved in the solution and could induce the morphology variations. In Figure 8 we observe the confocal Raman images of a biomorph growth in a gas diffusion experiment with PA added at the bottom of the mushroom. Similarly, as the previous result, it was monitored (ii) the $BaCO_3$ peak at 1062 cm^{-1}, (iii) the substrate glass between 515 and 620 cm^{-1}; and (iv) amorphous SiO_2 between 440 and 520 cm^{-1}. These results show congruence with the obtained when using Sr as alkaline earth metal in the formation of biomorphs (Supplementary materials, Figure S4).

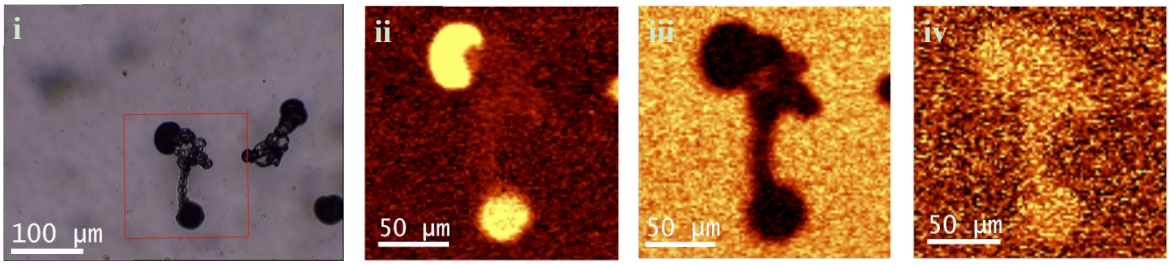

Figure 8. (**i**) Optical image of a Ba biomorph. (**ii**) Mapping of the 1062 cm^{-1} shift for $BaCO_3$ (**iii**) Mapping of the substrate glass tracked between 515 and 620 cm^{-1}. (**iii**) Amorphous SiO_2, tracked between 440 and 520 cm^{-1}.

5. Conclusions

In summary, we demonstrated that pyruvic acid, which is presumably an important compound involved in prebiotic ancient metabolic pathways, can induce the morphogenesis of typical biomorphs grown by gas diffusion and single-phase methods. In the first case, when PA [0.1 M] was added to a gas diffusion experiment, spherulitic structures were observed. When adding the PA to the bottom of the mushroom and sealed to environmental CO_2, we observed a mix between classical biomorphs and spherulitic structures which demonstrates that the photolysis of PA under UV produced a source of CO_3^{2-} ions, which led to the formation of alkaline earth metals precipitates in absence of atmospheric CO_2. In contrast with previous reports where Na_2CO_3 was used as source of carbonate ions, the degradation of PA enables the precipitation of carbonates in a similar temporal regime as that in the gas diffusion method, without the inconvenient delay of several days to observe the biomorphs' growth when carbonate salts are used. Finally, when PA was added to the sol and sealed from atmospheric gas diffusion simulating a single phase experiment, spherulitic precipitates, similar to those in the gas diffusion setup exposed to environmental CO_2, are formed. The smoothed surfaces observed suggest the partial inhibition of carbonate precipitation and possible the favoring of a laminar cover of amorphous silica on the initial $BaCO_3$ crystalline arrangement. These observations support earlier asseverations regarding the importance of local pH at the front of the growth. Nonetheless, the unresolved question that remains is if the morphogenesis of Ba and Sr biomorphs is due to either the absorption of molecules on the precipitate's surface, or if it is accounted to the local pH gradient.

Supplementary Materials: The following are available online at http://www.mdpi.com/2073-4352/9/2/67/s1, Figure S1. Scanning electron microscopy (SEM) images of silica-carbonate biomorphs synthetized with Sr. (**a**) Control sample without PA; (**b**) PA [0.01 M]; (**c**) PA [0.1 M]. Figure S2. Energy dispersion spectroscopy (EDS) from: Top: a control sample of Ba silica-carbonate biomorph. Bottom: a Ba silica-carbonate spherulitic structure synthetized in gas-diffusion under UV radiation. Figure S3. Raman spectrum from the glass substrate. Figure S4. Confocal Raman imaging of Sr biomorphs synthetized with PA [0.1 M]. (**a**) Gas-diffusion method under UV radiation; (**b**) single-phase method under UV radiation. (i) Optical image of the structure; (ii) mapping of the $SrCO_3$ peak at 1070 cm^{-1}; (iii) mapping of the SiO_2 between 515 and 620 cm^{-1}.

Author Contributions: Conceptualization, A.M. and K.S.P.; methodology, K.S.P.; writing—review and editing, A.M. and K.S.P.; funding acquisition, A.M.

Acknowledgments: Authors acknowledge to CONACYT, for the Postdoctoral Fellowship, grant No. 291159, to Karina S. Pérez and to DGAPA-UNAM for the support through DGAPA UNAM PAPIIT project No. IG200218. Also we thank to the Laboratorio Universitario de Caracterización Espectroscópica, LUCE_ICAT_UNAM, and to Selene Islas for the Confocal Raman Microscopy measurements. We are grateful with Carlos Magaña Zavala and Samuel Tehuacanero Cuapa for the EDS characterization at IFUNAM.

Conflicts of Interest: The authors declare no conflict of interest. The funders had no role in the design of the study; in the collection, analyses, or interpretation of data; in the writing of the manuscript, or in the decision to publish the results.

References

1. Schopf, J.W. *Earth's Earliest Biosphere*; Princeton University Press: Princeton, NJ, USA, 1983.
2. García-Ruiz, J.M. Inorganic self-organisation in precambrian cherts. *Orig. Life Evol. B* **1994**, *24*, 451–467. [CrossRef]
3. García-Ruiz, J.M.; Carnerup, A.; Christy, A.G.; Welham, N.J.; Hyde, S.T. Morphology: An Ambiguous Indicator of Biogenicity. *Astrobiology* **2002**, *2*, 353–369. [CrossRef] [PubMed]
4. Hyde, S.T. Crystals: Animal, vegetable or mineral? *Interface Focus* **2015**, *5*, 20150027. [CrossRef] [PubMed]
5. Lowenstam, H.A. Minerals formed by organisms. *Science* **1981**, *211*, 1126–1131. [CrossRef] [PubMed]
6. Weiner, S. Biomineralization: A structural perspective. *J. Struct. Biol.* **2008**, *163*, 229–234. [CrossRef] [PubMed]
7. García-Ruiz, J.M. Teoría del crecimiento de cristales en geles. Precipitación polimórfica y agregados cristalinos de morfología inducida. Ph.D. Thesis, Universidad Complutense, Madrid, Spain, 1980.
8. García-Ruiz, J.M.; Amorós, J.L. Morphological aspects of some symmetrical crystal aggregates grown by silica gel technique. *J. Cryst. Growth* **1981**, *55*, 379–383. [CrossRef]
9. Baird, T.; Braterman, P.S.; Chen, P.; García-Ruiz, J.M.; Peacock, R.D.; Reid, A. Morphology of gel-grown barium carbonate aggregates—pH effect on control by silicate-carbonate membrane. *Mater. Res. Bull.* **1992**, *27*, 1031–1040. [CrossRef]
10. Bittarello, E.; Aquilano, D. Self-assembled nanocrystals of barium carbonate in biomineral-like structures. *Eur. J. Mineral.* **2007**, *19*, 345–351. [CrossRef]
11. Noorduin, W.L.; Grinthal, A.; Mahadevan, L.; Aiznberg, J. Rationally Designed Complex, Hierarchical Microarchitectures. *Science* **2013**, *340*, 832–837. [CrossRef]
12. Nakouzi, E.; Knoll, P.; Hendrix, K.B.; Steinbock, O. Systematic characterization of polycrystalline silica-carbonate helices. *Phys. Chem. Chem. Phys.* **2016**, *18*, 23044–23052. [CrossRef]
13. Nakouzi, E.; Steinbock, O. Self-organization in precipitation reactions far from the equilibrium. *Sci. Adv.* **2016**, *2*, e1601144. [CrossRef]
14. Kellermeier, M.; Eiblmeier, J.; Melero-García, E.; Pretzl, M.; Fery, A.; Kunz, W. Evolution and Control of Complex Curved Form in Simple Inorganic Precipitation Systems. *Cryst. Growth Des.* **2012**, *12*, 3647–3655. [CrossRef]
15. Sánchez-Puig, N.; Guerra-Flores, E.; López-Sánchez, F.; Juárez-Espinoza, P.A.; Ruíz-Arellano, R.; González-Muñoz, R.; Arreguín-Espinosa, R.; Moreno, A. Controlling the morphology of silica-carbonate biomorphs using proteins involved in biomineralization. *J. Mater. Sci.* **2012**, *47*, 2943–2950. [CrossRef]
16. Opel, J.; Wimmer, F.P.; Kellermeier, M.; Cölfen, H. Functionalisation of silica-carbonate biomorphs. *Nanoscale Horiz.* **2016**, *1*, 144–149. [CrossRef]
17. Saladino, R.; Botta, G.; Bizarri, B.M.; Di Mauro, E.; García-Ruíz, J.M. A Global Scale Scenario for Prebiotic Chemistry: Silica-Based Self-Assembled Mineral Structures and Formamide. *Biochemistry* **2016**, *55*, 2806–2811. [CrossRef] [PubMed]
18. Hazen, R.M.; Deamer, D.W. Hydrothermal Reactions of Pyruvic Acid: Synthesis, Selection, and Self-Assembly of Amphiphilic Molecules. *Orig. Life Evol. Biosph.* **2007**, *37*, 143–152. [CrossRef] [PubMed]
19. Guzmán, M.I.; Colussi, A.J.; Hoffmann, M.R. Photoinduced Oligomerization of Aqueous Pyruvic Acid. *J. Phys. Chem. A* **2006**, *110*, 3619–3626. [CrossRef]
20. Lim, H.-J.; Carlton, A.G.; Turpin, B.J. Isoprene Forms Secondary Organic Aerosol through Cloud Processing: Model Simulations. *Environ. Sci. Technol.* **2005**, *39*, 4441–4446. [CrossRef]

21. Carlton, A.G.; Turpin, B.J.; Lim, H.J.; Altieri, K.E.; Seitzinger, S. Link between isoprene and secondary organic aerosol (SOA): Pyruvic acid oxidation yields low volatility organic acid in clouds. *Geophys. Res. Lett.* **2006**, *33*, L06822. [CrossRef]
22. Harris, A.E.R.; Cazaunau, M.; Gratien, A.; Pangui, E.; Doussin, J.-F.; Vaida, V. Multiphase Photochemistry of Pyruvic Acid under Atmospheric Conditions. *J. Phys Chem. A* **2017**, *121*, 3327–3339. [CrossRef]
23. Lin, C.-C.; Liu, L.-G. Post-Aragonite Phase-Transitions in Strontianite and Cerussite—A High-Pressure Raman Spectroscopy Study. *J. Phys. Chem. Solids* **1997**, *58*, 977–987. [CrossRef]
24. Kuo, S.-C.; Tsai, Y.I.; Tsai, C.-H.; Hsieh, L.-Y. Carboxylic acids in $PM_{2.5}$ over *Pinus* morrisonicola forest and related photoreaction mechanisms identified via Raman spectroscopy. *Atmos. Environ.* **2011**, *45*, 6741–6750. [CrossRef]
25. Opel, J.; Hecht, M.; Rurack, K.; Eiblmeier, J.; Kunz, W.; Cölfen, H.; Kellermeier, M. Probng local pH-based precipitation processes in self-assembled silica-carbonate hybrid materials. *Nanoscale* **2015**, *7*, 17434–17440. [CrossRef] [PubMed]
26. Eiblmeier, J.; Kellermeier, M.; Deng, M.; Kienle, L.; García-Ruiz, J.M.; Kunz, W. Bottom-Up Self-Assembly of Amorphous Core-Shell-Shell Nanoparticles and Biomimetic Crystal Forms in Inorganic Silica-Carbonate Systems. *Chem. Mater.* **2013**, *25*, 1842–1851. [CrossRef]
27. García-Ruiz, J.M.; Nakouzi, E.; Kotopoulou, E.; Tamborrino, L.; Steinbock, O. Biomimetic mineral self-organization from silica-rich spring waters. *Sci. Adv.* **2017**, *3*, e1602285. [CrossRef] [PubMed]
28. Ruiz-Arellano, R.R.; Moreno, A. Obtainment of Spherical-Shaped Calcite Crystals Induced by Intramineral Proteins from Eggshells of Ostrich and Emu. *Cryst. Growth Des.* **2014**, *14*, 5137–5143. [CrossRef]
29. Nakouzi, E.; Knoll, P.; Steinbock, O. Biomorph growth in single-phase systems: Expanding the spectrum and pH range. *Chem. Commun.* **2016**, *52*, 2107–2110. [CrossRef] [PubMed]
30. Grgić, I.; Nieto-Gligorovski, L.I.; Net, S.; Temime-Roussel, B.; Gligorovski, S.; Wortham, H. Light induced multiphase chemistry of gas-phase ozone on aqueous pyruvic and oxalic acids. *Phys. Chem. Chem. Phys.* **2010**, *12*, 698–707. [CrossRef]
31. Altieri, K.E.; Carlton, A.G.; Lim, H.-J.; Turpin, B.J.; Seitzinger, S.P. Evidence for oligomer formation in clouds: Reactions of isoprene oxidation products. *Environ. Sci. Technol.* **2006**, *40*, 4956–4960. [CrossRef]
32. Rouillard, J.; García-Ruiz, J.M.; Gong, J.; van Zuilen, M.A. A morphogram for silica-witherite biomorphs and its application to microfossil identification in the early earth rock record. *Geobiology* **2018**, *16*, 279–296. [CrossRef]